RSC Advances

PAPER

View Article Online
View Journal | View Issue

Cite this: *RSC Adv.*, 2019, **9**, 27996

Unorthodox synthesis, biological activity and DFT studies of novel and multifunctionalized naphthoxocine derivatives†

Mohamed Ahmed Abozeid,[a] Aya Atef El-Sawi,[a] Mohamed Ramadan Elmorsy,[a] Mohamed Abdelmoteleb,[bc] Abdel-Rahman Hassan Abdel-Rahman[a] and El-Sayed Ibrahim El-Desoky *[a]

Received 7th July 2019
Accepted 29th August 2019

DOI: 10.1039/c9ra05154f

rsc.li/rsc-advances

A new promising protocol has been developed for the synthesis of scarce oxocine derivatives **3a–e** and **6** through addition of amine-based nucleophiles such as hydroxylamine hydrochloride, primary amine and hydrazide to chromonylidene benzothiazol-2-ylacetonitrile **2** in refluxing dioxane under metal free reaction conditions in moderate to good yields. Other nitrogen nucleophiles such as piperidine, hydrazine and thiosemicarbazide failed to afford the corresponding oxocinols, and instead pyridine derivatives **7**, **8** and **10** were obtained exclusively. Predictive study for the biological activities using PASS (prediction of activity spectra for biologically active substances) online software showed optimistic activities for oxocinols **3a–e** in the treatment of cancer, influenza A and microbial infections. Additionally, DFT studies of oxocine derivatives **3a–e** and **6** indicated the presence of required thermodynamics parameters for the application in dye-sensitized solar cells (DSSCs).

Introduction

The medium sized (7 to 9 membered) cyclic ethers are biologically interesting as well as challenging organic skeletons due their occurrence in numerous bioactive natural products in addition to their complex and macrocyclic structure which hinder their synthesis.[1] In this class of macro- and heterocycles, oxocine constitutes a common scaffold in different biologically active natural products such as heliannoul H, acremine G and protosapannin B in addition to alkaloids such as murraya and arcyroxocin (Fig. 1).[2–8]

Consequently, many chemists have paid increased attention to develop new methodologies in order to build up this promising scaffold over the last ten years such as (1) retro-Claisen rearrangement,[9] (2) ring closing olefin metathesis[10] (3) Ni-catalyzed reductive Heck reaction,[6] (4) DABCO-mediated [4+4] domino annulation of ynone and α-cyano-α,β-unsaturated ketone,[7] (5) Lewis acid promoted acetal–alkene cyclization,[11] and others.[12–23] However, even in the presence of these various protocols, many observable drawbacks have been encountered such as applying drastic conditions, using precious heavy metal catalysts, needing to have finely designed starting materials and tedious purification. Therefore, it would be worthy to develop new cost effective and functional group tolerant synthetic methodology toward oxocine framework.

In the view of the aforementioned natural occurrence and biological importance of oxocine heterocyclic compounds, we herein report our recent findings in the synthesis of oxocine derivatives *via* simple and novel domino nucleophilic addition of amine-based nucleophiles to chromonylidene benzothiazol-2-ylacetonitrile **2** affording the corresponding oxocine derivatives **3a–e** and **6** in moderate to good yields.

Results and discussion

Chemistry

The acid mediated condensation of formylbenzochromone **1** (ref. 24) with 2-cyanomethyl-1,3-benzothiazole afforded the corresponding *E*,*Z*-mixture of 2-cyano-2-(1,3-benzothoazol-2-yl)-3-vinylnaphthopyran-4-one (**2**) in 90% yield (Scheme 1). Under

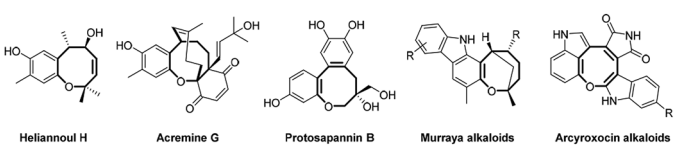

Fig. 1 Representative examples of biologically active oxocine natural products.

[a]*Department of Chemistry, Faculty of Science, Mansoura University, Mansoura-35516, Egypt. E-mail: prof.desoky.orgchem@gmail.com; Fax: +20502246254; Tel: +201060614054*

[b]*Food Allergy Research & Resource Program (FARRP), Department of Food Science & Technology, University of Nebraska, Lincoln, NE, USA*

[c]*Department of Botany, Faculty of Science, Mansoura University, Mansoura-35516, Egypt*

† Electronic supplementary information (ESI) available. See DOI: 10.1039/c9ra05154f

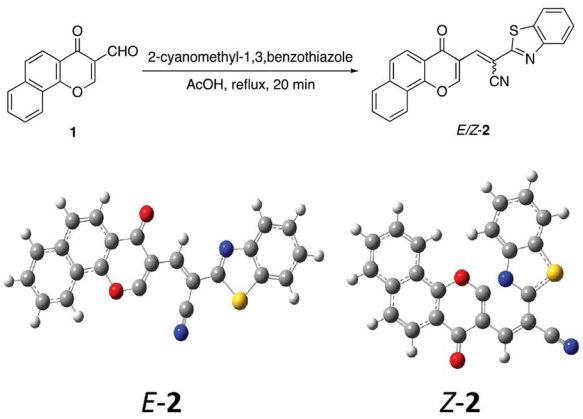

Scheme 1 Synthesis and energy-optimized geometrical structures of *E*- and *Z*-chromonylidene **2**.

acidic reaction conditions, equimolar *E*,*Z*-mixture of chromonylidene benzothiazol-2-ylacetonitrile **2** was obtained. The formation of both isomers in almost equal amounts might be rationalized to the absence of energy barrier between both isomers due to the presence of bulky 1,3-benzothiazole heterocyclic moiety. This assumption was further supported by DFT studies of the optimized geometrical structures of *E*-**2** and *Z*-**2** as shown in Scheme 1. The calculations were computed by Gaussian 09 software using B3LYP as functional energy and 6-31G (d,p) as a basis set,[25–28] revealed the equal energies of both geometrical isomers (−1532.9 au for *E*-**2** and −1533 au for *Z*-**2**).

Based on the skeletal features of the key compound **2**, we hypothesized the pathway shown in Scheme 2 towards oxocine skeleton. In order to build up this 8-membered heterocycle, our hypothesis was based upon creating a new connectivity between the oxygen pro-nucleophile and cyano electrophilic position. In order to unveil the oxygen nucleophile, the γ-pyrone ring has to be opened using some nucleophile to generate free hydroxyl group as shown in intermediate **B** (Pathway a). After that, the *in situ* generated hydroxyl group will attack cyano group to give the desired oxocine skeleton. Actually, this process most probably will be accompanied by various side reactions (for example: Pathways b and c) due to the presence of different nucleophiles which can easily attack the cyano group as well.

In order to test the possibility of our hypothesis, we selected the reaction of chromonylidene benzothiazol-2-ylacetonitrile **2** with

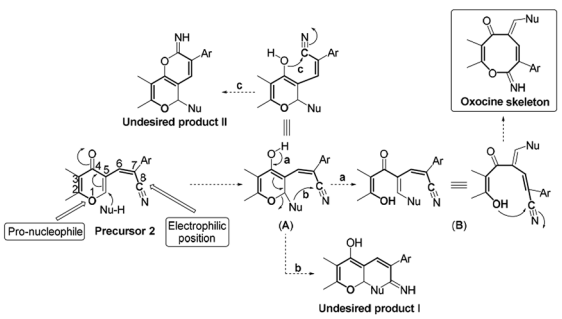

Scheme 2 Working hypothesis.

hydroxylamine hydrochloride to build up the oxocinol heterocycle **3a** (Table 1). However, no reaction was observed by boiling **2** with hydroxylamine hydrochloride in ethanol (Entry 1), trace amount of the desired product **3a** was detected by performing the reaction in 1,4-dioxane at 80 °C (Entry 2). By increasing the temperature to 101 °C, the desired product **3a** was isolated in 55% yield (Entry 3). Additionally, the use of other solvents with increasing boiling points failed to improve the yield of **3a** (Entries 4–8). The attempts by using different organic and inorganic basic additives failed to increase the chemical yield as well (Entries 9–13). Moreover, the use of basic additives promoted different reaction pathways and leaded to tedious chromatographic purification of **3a** (Entries 9–13). Increasing the amount of hydroxylamine hydrochloride (1.5 equivalent) didn't impart any benefits (Entry 14).

The skeleton of oxocinol **3a** was secured based upon different analytical analyses. Firstly, IR spectrum showed absorption peaks at regions 3430–3570, 3319 and 3198 cm^{-1} assigned for two OH's and NH groups. In addition, ^1H NMR spectrum of **3a** showed two characteristic singlets at 8.78 and 8.83 ppm which were assigned to protons CH=N and H-4 (oxocinol), respectively. The ^{13}C NMR spectrum of **3a** exhibited all carbons of the proposed structure. EI-MS supported the proposed structure of compound **3a** by the presence of molecular ion peak at *m*/*z* 413, which was compatible with its molecular weight. The formation of side products **4** (ref. 29) and **5** (ref. 30) was excluded due to the absence of aliphatic CH in ^1H- and ^{13}C-NMR.

Table 1 Optimization of the reaction conditions[a]

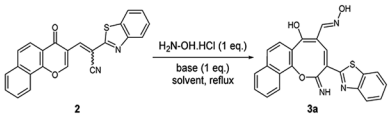

Entry	Solvent	Temp. °C	Base	Time	Yield (%)
1	Ethanol	78	None	12 h	NR[b]
2	1,4-Dioxane	80	None	12 h	Trace
3	1,4-Dioxane	101	None	30 min	55
4	Isobutanol	108	None	3 h	30
5	Toluene	111	None	6 h	12
6	Pyridine	115	None	1 h	45
7	TCE[c]	121	None	12 h	NR[b]
8	DMF[d]	153	None	12 h	ND[e]
9	1,4-Dioxane	101	Et_3N	30 min	41
10	1,4-Dioxane	101	DBU	5 min	22
11	1,4-Dioxane	101	NaOAc	30 min	41
12	1,4-Dioxane	101	K_2CO_3	1.5 h	40
13	1,4-Dioxane	101	NaOH	10 min	47
14[f]	1,4-Dioxane	101	None	30 min	55

Possible side products

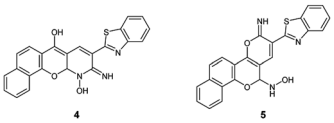

[a] Reaction conditions: **1** (1 mmol) and hydroxylamine·HCl (1 mmol) in 15 ml solvent. [b] NR: no reaction. [c] TCE: tetrachloroethylene. [d] DMF: *N*,*N*-dimethylformamide. [e] ND: not detected. [f] Using hydroxylamine·HCl (1.5 eq.).

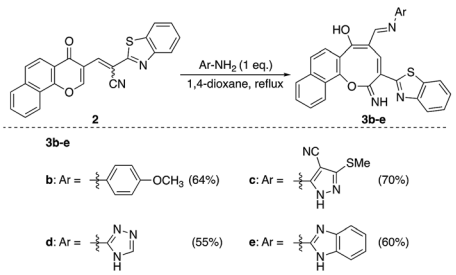

Scheme 3 Reaction of chromonylidene **2** with different 1° amines.

Similarly, the newly developed methodology could be applied with different primary homo and heteroaryl amines such as *p*-ansidine, 5-amino-3-methylthio-1*H*-pyrazole-4-carbonitrile, 2-amino-1,3,4-triazole and 2-amino benzimidazole affording the corresponding oxocinol products **3b–e** in moderate to good yields (Scheme 3).

Additionally, the reaction of **2** with cyanoacetic acid hydrazide in the presence of a catalytic amount of triethylamine afforded oxocinone **6** in 50% yield (Scheme 4). This reaction involved initially the aforementioned cascade process to build up the corresponding oxocinol intermediate **I** which underwent enol to keto tautomerization giving intermediate **II**, form which the final product **6** was formed by further cyclization between hydrazonyl NH and cyano group (Scheme 4). IR spectrum of oxocinone **6** confirmed the absence of cyano group, and instead hydroxyl group was observed at 3550–3420 cm^{-1} as broad peak in addition to aliphatic CH functionality peaks at 2961, 2898 cm^{-1}. The ^1H NMR analysis showed a singlet at δ 4.25 ppm assignable to methylene protons of pyrazole ring.

On the other hand, the reaction of chromonylidene **2** with piperidine in refluxing 1,4-dioxane didn't afford the corresponding oxocinol product, and instead, 2-(benzo[*d*]thiazol-2-yl)-12-(piperidin-1-yl)-4,12-dihydro-3*H*-benzo[7,8]chromeno[4,3-*b*]pyridine-3-one (**7**) was obtained in 66% yield (Scheme 5). The formation of pyridinone **7** was proposed to proceed *via* nucleophilic attack at C-2 of γ-pyrone accompanied by the generation hydroxyl group at C-4 (intermediate **I**), which attack the nearby cyano group giving α-iminopyrone intermediate **II**. By Dimroth rearrangement, α-iminopyrone intermediate **II** was transformed into the corresponding product **7**. The IR spectrum of pyridinone **7** showed a broad peak at 3350–3460 cm^{-1} which was attributable to NH group in addition to the amidic carbonyl peak at 1643 cm^{-1}. Additionally, the newly inserted aliphatic carbons of piperidinyl moiety were expressed in IR by the peaks at the range of 2931–2816 cm^{-1}. The ^1H NMR spectrum of compounds **7** showed a characteristic singlet δ 6.97 ppm assigned to the methine proton (H-5). In a different scenario, no

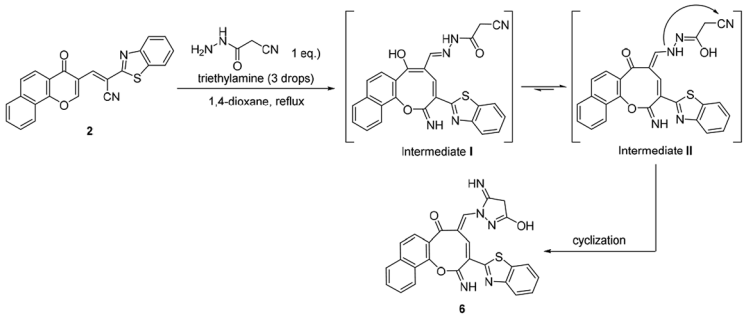

Scheme 4 Reaction of chromonylidene **2** with cyanoacetic acid hydrazide.

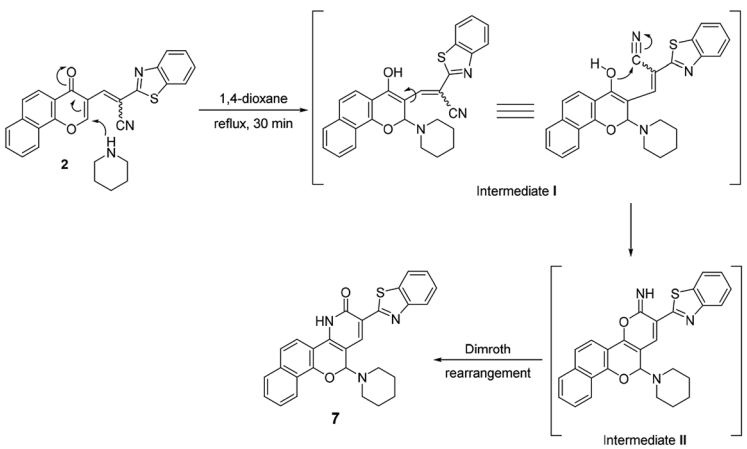

Scheme 5 Reaction of chromonylidene **2** with piperidine.

reaction was observed in the case of the reaction of chromonylidene **2** with triethylamine (3° amine) even after prolonged reaction time (12 h).

Moreover, the reaction of chromonylidene **2** with hydrazine hydrate in refluxing 1,4-dioxane afforded product **8** (73% yield) which was generated in a completely different scenario to the aforementioned reactions with primary and secondary amines (Scheme 6). Treatment of precursor **2** with thiosemicarbazide produced the ring junction nitrogen product **10** in 53% yield as shown in the reaction pathway (Scheme 7). The reaction proceeded in a similar style to the reaction with hydrazine hydrate (Scheme 6).

The different reaction profiles of chromonylidene **2** with hydroxyl amine and its similar nucleophiles (products **3a–e** and **6**) compared to hydrazine nucleophile (product **8**) were explained on the basis of the electron density on the nucleophilic centers in the corresponding intermediates **B** (Fig. 2). These electron densities were measured on the optimized structures using Gaussian 09 software at DFT level *via* B3LYP as energy function and 6-31G (d,p) as a basis set.[25–28] In the case of key intermediate for oxocinol **3a**, the electron density on phenolic OH group was found to be (−0.61 e) which is higher than the corresponding density on NH group (−0.47 e). This significant difference in the electron density value enhanced the nucleophilicity of phenolic OH compared to that of NH group leading to the desired oxocine derivatives **3a–e** and **6.** In the case of key intermediate for pyridine **8,** the electron density on NH center was increased due to the presence of adjacent NH_2 group to value of −0.58 e which became very close to the value of phenolic OH group. As a result, the 6-membered cyclization (affording product **8**) became more energetically favored than 8-membered cyclization (affording product **9**). In the case of the reaction with thiosemicarbazide (Scheme 7), the calculated electron densities on the nucleophilic centers could not rationalize solely the formation of product **10** where its formation might be attributed to some other thermodynamic parameters.

Computational prediction of biological activities of oxocine derivatives 3a–e and 6

PASS online software was used to predict the putative biological activity spectrum of the oxocine derivatives **3a–e** and **6** which was represented in Table 2. From the results of biological activity prediction, the synthesized oxocine derivatives **3a–e** and **6** showed various anticancer (antimetastatic, anti-ischemic (cerebral), antineoplastic, and protection from

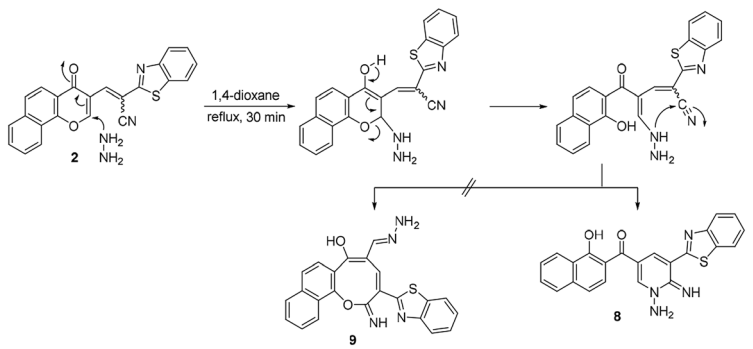

Scheme 6 Reaction of chromonylidene **2** with hydrazine hydrate.

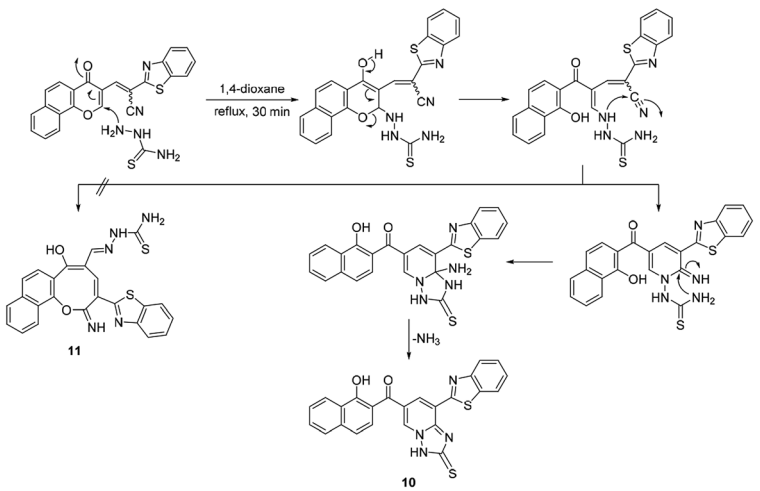

Scheme 7 Reaction of chromonylidene **2** with thiosemicarbazide.

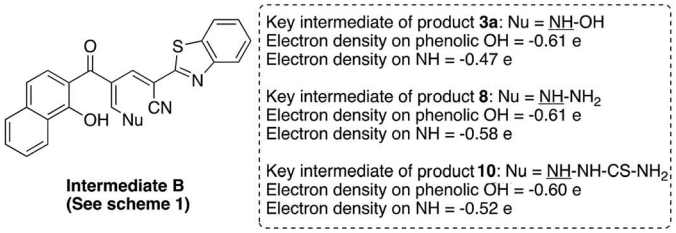

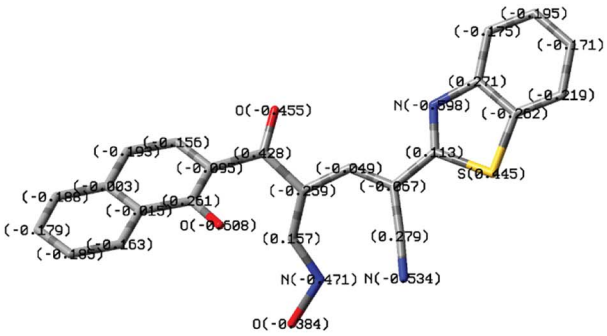

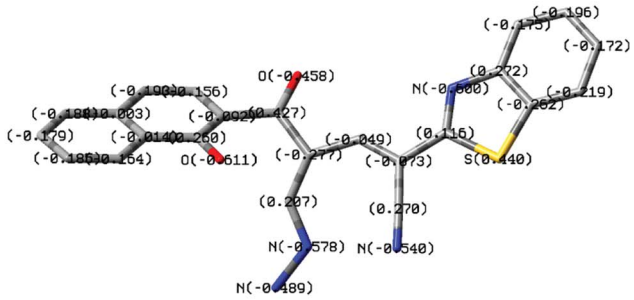

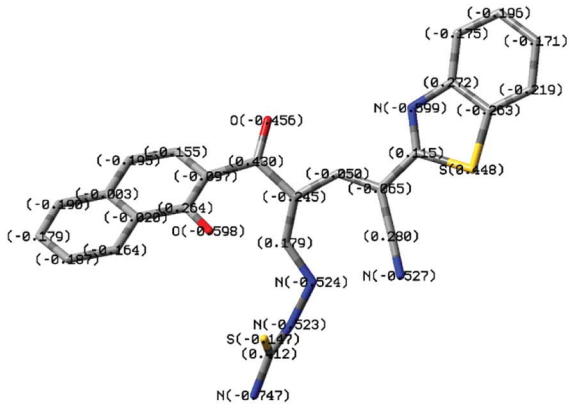

Fig. 2 Electron densities on OH and NH functionalities of the key intermediate B in case of products 3a, 8 and 10.

Table 2 Biological activity assessment using PASS online software

		3a		3b		3c		3d		3e		6	
Biological activity		Pa	Pi	Pa	Pi	Pa	Pi	Pa	Pi	Pa	Pi	Pa	Pi
Anticancer	Antimetastatic	NA	NA	0.310	0.077	0.238	0.119	0.201	0.158	0.220	0.135	0.212	0.143
	Antiischemic (cerebral)	0.472	0.125	0.378	0.204	NA	NA	0.414	0.174	NA	NA	0.503	0.104
	Antineoplastic	0.604	0.044	0.640	0.037	0.492	0.074	0507	0.069	0.468	0.081	0.565	0.053
	Antineoplastic (brain cancer)	NA	NA	0.226	0.084	0.198	0.133	0212	0.108	0.202	0.126	NA	NA
	Prostate cancer treatment	0.515	0.008	0.511	0.009	0.343	0.031	0.459	0.014	0.480	0.012	0.459	0.014
Antiviral	Influenza A	0.245	0.106	0.214	0.181	0.242	0.112	0.536	0.004	0.549	0.004	0.417	0.007
Antimicrobial	Antibiotic	0.183	0.033	0.254	0.019	0.147	0.051	0.181	0.034	0.176	0.036	0.169	0.039
	Antibacterial	0.358	0.041	0.487	0.018	0.258	0.079	0.359	0.041	0.306	0.058	0.275	0.070

prostate cancer), antiviral, and antimicrobial promising activities. Oxocinols **3a** and **3b** showed the best probable activity in the treatment of cancer. In addition, oxocinol **3b** revealed the best predicted antimicrobial activity. Ultimately, compounds **3d** and **3e** may possess antiviral (influenza A) activity.

Applications of oxocine derivatives 3a–e and 6 in dye-sensitized solar cells (DSSCs)

DFT calculations followed by TD-DFT studies were performed for oxocine derivatives **3a–e** and **6** using B3LYP as energy function and 6-31G (d,p)[25–28] as a basis set to investigate their theoretical GSOP/ESOP energy levels (Fig. 3) and their optical absorption spectra (Fig. 4).[31]

In addition, from the results displayed in Table 3, it is quite interesting to note that, all products **3a–e** and **6** possess the thermodynamic requirements as an application for DSSCs.[32,33] The estimated ESOP levels of **3a–e** and **6** were found to be **3a** (−3.13 eV), **3b** (−2.66 eV), **3c** (−2.76 eV), **3d** (−3.12 eV), **3e** (−2.41 eV) and **6** (−3.02 eV). These values are more positive than the conduction band (CB) potential of TiO_2 (−4.2 eV); showing that their ability for the electron injection. Furthermore, the calculated GSOP/HOMO levels of

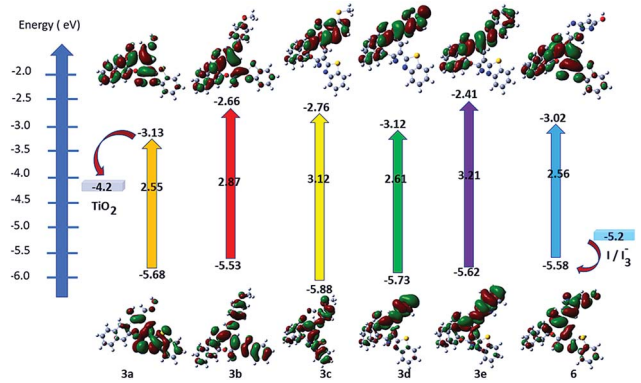

Fig. 3 Energy level diagram of oxocine derivatives **3a–e** and **6**.

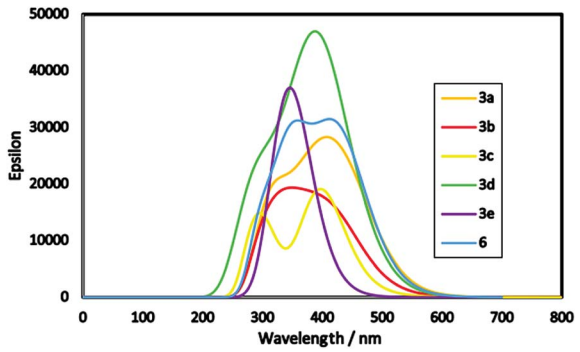

Fig. 4 Simulated absorption spectra of oxocine derivatives **3a–e** and **6**.

Table 3 Calculated E_{0-0}, GSOP and ESOP for oxocine derivatives **3a–e** and **6**

Product	Basis set	GSOP (eV)	E_{0-0}	ESOP (eV)
3a	B3LYP/6-31G (d,p)	−5.68	2.55	−3.13
3b		−5.53	2.87	−2.66
3c		−5.88	3.12	−2.76
3d		−5.73	2.61	−3.12
3e		−5.62	3.21	−2.41
6		−5.58	2.56	−3.02

3a (−5.68 eV), **3b** (−5.53 eV), **3c** (−5.88 eV), **3d** (−5.73 eV), **3e** (−5.62 eV) and **6** (−5.68 eV) were found to be more negative than the oxidation potential of the electrolyte (−5.2 eV) (I_3^-/I^-), exhibited the regeneration of the electrons.

Furthermore, energy band gap (E_{0-0}) can be estimated from the onset of the lowest energy peak.[34] Small band gap increases the optical properties of the products allowing for absorption most of the incident light. From Fig. 4, product **3a** is found to be red shifted than other products which attributed to its lowest optical energy gap of 2.55 eV. Moreover, molar extinction coefficient (epsilon) plays a vital role for enhancing the light harvesting ability of the dye where its higher value indicates maximum light harvesting capability. For example, product **3d** showed the highest molar extinction co-efficient with broadening in its absorption peak depending on the nature of its donor and acceptor structures, and as a result it is expected to show improved photovoltaic performance in DSSCs.[35]

Conclusion

A promising protocol for the synthesis of oxocine derivatives **3a–e** and **6** has been developed *via* reaction of chromonylidene **2** with different NH_2 bearing nucleophiles under metal free conditions refluxing in 1,4-dioxane. Other nucleophiles such as piperidine, hydrazine and thiosemicarbazide failed to give the desired oxocine derivatives and instead, they afforded different pyridine derivatives **7**, **8** and **10**. Some oxocine products showed some promising probability of biological activity in the treatment of cancer, influenza A, and as antimicrobial agents. Furthermore, TD-DFT simulated spectra and calculated GSOP/ESOP energy levels indicated the ability of using products **3a–e** and **6** in the application of DSSCs. The present study is just preliminary where detailed studies for the synthesis of different oxocine derivatives in addition to biological activity and DSSCs applications are currently underway, with collaboration with different specialized research groups, and will be reported in the due time.

Experimental

General

The melting points of the newly synthesized compounds were measured on a Gallenkamp electrical melting point apparatus using open glass capillaries and are reported in degree Celsius (°C) (uncorrected). The infrared spectra (IR) were determined using the pressed KBr disc method on a Mattson 5000 FT-IR spectrophotometer (Faculty of Pharmacy, Mansoura University) or Nicolet iS10 FT-IR Spectrometer (Faculty of Science, Mansoura University). The ^{1}H-NMR spectra were measured on Bruker AC 300 MHz (Faculty of Science, Cairo University), Bruker Avance III 400 MHz (Faculty of Pharmacy, Beni Suef University) and/or JEOL ECA II 500 MHz (Faculty of Science, Mansoura University) using tetramethylsilane (TMS) as an internal reference, and using DMSO-d_6 or trifluoroacetic acid (TFA) as solvents. The signals' multiplicities are reported as follows: s = singlet, d = doublet, dd = doublet of doublets and m = multiplet. Exchangeable protons were detected through D_2O test. ^{13}C-NMR spectra were measured on JEOL ECA II 125 MHz (Faculty of Science, Mansoura University). The electron impact mass spectra (EI-MS) were determined on Thermo Fisher scientific DSQ II GC/MS with focus GC (70 eV) (Faculty of Science, Mansoura University) or Kratos MS (70 eV) equipment (Faculty of Pharmacy, Al-Azhar University). Elemental analysis was executed at the microanalytical lab at Cairo University. All reactions were monitored using thin layer chromatography (TLC) on aluminum sheets pre-coated with Al_2O_3 with fluorescent indicator F254, Merck (Darmstadt, Germany). DFT-followed by TD-DFT were performed using Gaussian 09 package software. The simulated absorption spectra of products **3a–e** and **6** obtained at B3LYP/6-31G (d,p) level.

Synthesis

Synthesis of 2-(benzo[*d*]thiazol-2-yl)-3-(4-oxo-4*H*-benzo[*h*]chromen-3-yl)acrylonitrile (2).

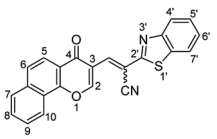

A mixture of 3-formylbenzochromone (673 mg, 3 mmol), 2-benzothiazoleacetonitrile (523 mg, 3 mmol) in glacial acetic acid (25 ml) was refluxed for 20 min. The formed precipitate was filtered off and recrystallized from a mixture of DMF/EtOH giving product **2** ($E:Z = 1:1$). Yield (1027 mg, 90%); reddish orange crystals; mp = 286–288 °C; IR (KBr, ν/cm^{-1}): 3061 (aromatic CH), 2206 (CN), 1650 (C=O), 1603 (C=N); ^{1}H NMR (500 MHz, DMSO-d_6): δ (ppm) 7.40 (s, 1H, H-2$_a$),7.52 (dd, 1H, H-6′$_a$, J = 7.00, 8.00 Hz), 7.55 (d, 1H, H-7′$_a$, J = 8.20 Hz), 7.60–7.67 (m, 4H, Ar–H), 7.73 (dd, 1H, H-6′$_b$, J = 7.50, 8.00 Hz),7.85–7.91 (m, 3H, Ar–H), 7.93 (d, 1H, H-7′$_b$, J = 8.20 Hz), 8.00 (d, 2H, Ar–H, J = 8.90 Hz), 8.04 (s, 1H, H-2$_b$),8.05 (d, 1H, Ar–H, J = 8.90 Hz), 8.10–8.18 (m, 4H, Ar–H), 8.22 (d, 1H, H-10$_a$, J = 7.60 Hz), 8.35 (s, 1H, CH$_a$=C–CN), 8.57 (d, 1H, H-10$_b$, J = 7.60 Hz), 9.46 (s, 1H, CH$_b$=C–CN); EI-MS m/z (%): 382.14 [M$^+$ + 2] (11.91), 381.19 [M$^+$ + 1] (29.07), 380.20 [M$^+$] (100.00), 352.22 (30.16), 351.19 (94.43), 350.30 (11.86), 114.12 (26.95); anal. calcd for $C_{23}H_{12}N_2O_2S$ (380.06): C, 72.62; H, 3.18; N, 7.36; S, 8.43%. Found: C, 72.65; H, 3.20; N, 7.32; S, 8.50%.

General procedure for the synthesis of compounds 3a–e, 6–8 and 10. A suspension of compound **2** (380 mg, 1 mmol) and nitrogen nucleophilic component (1 mmol) such as [hydroxylamine·HCl, *p*-anisidine, 5-amino-3-(methylthio)-1*H*-pyrazole-3-carbonitrile, 2-amino-1,3,4-triazole, 2-aminobenzimidazole, cyanoacetic acid hydrazide, piperidine, hydrazine hydrate, thiosemicarbazide] in 15 ml dry 1,4-dioxane was refluxed for 30 min (in the case of cyanoacetic acid hydrazide, 3 drops of Et_3N was added as catalyst). The formed precipitate was filtered off, washed several times with hot 1,4-dioxane followed by absolute EtOH to give the corresponding products without the need for further purification.

3-(Benzo[*d*]thiazol-2-yl)-6-hydroxy-2-imino-2*H*-naphtho[1,2-*b*]oxocine-5-carbaldehyde oxime (3a).

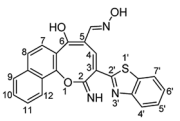

Yellow needles; (227 mg, 55%); mp > 330 °C; IR (KBr, ν/cm^{-1}): 3430–3570 (OH, broad), 3319 (NH), 3065 (aromatic CH),1627 (C=N), 1583 (C=C); ^{1}H NMR (500 MHz, TFA): δ (ppm) 7.45 (d, 1H, H-8, J = 8.70 Hz), 7.51 (d, 1H, H-7, J = 8.90 Hz), 7.66–7.72 (m, 2H, Ar–H), 7.75–7.82 (m, 2H, Ar–H), 7.87 (d, 1H, H-7′, J = 8.00 Hz), 8.09 (d, 1H, H-4′, J = 8.00 Hz), 8.22 (d, 1H, H-9, J = 8.00 Hz), 8.56 (d, 1H, H-12, J = 8.50 Hz), 8.78 (s, 1H, CH=N), 8.83 (s, 1H, H-4); ^{13}C NMR (126 MHz, TFA): δ (ppm) 119.10, 122.29, 123.51, 124.72, 125.06, 125.95, 126.11, 126.74, 128.99, 129.68, 130.01, 130.06, 133.99, 135.35, 140.41, 140.85, 141.76, 152.60, 153.17, 153.21, 163.29, 166.97, 194.84; EI-MS m/z (%): 415.18 [M$^+$ + 2] (5.69), 414.26 [M$^+$ + 1] (23.88), 413.22 [M$^+$] (85.42), 397.24 (100.00), 396.25 (41.78), 381.21 (25.85), 368.18 (7.77); anal. calcd for $C_{23}H_{15}N_3O_3S$ (413.45): C, 66.82; H, 3.66; N, 10.16; S, 7.75%. Found: C, 66.80; H, 3.69; N, 10.12; S, 7.79%.

3-(Benzo[*d*]thiazol-2-yl)-2-imino-5-((4-methoxyphenyl)imino)methyl-2*H*-naphtho[1,2-*b*]oxocin-6-ol (3b).

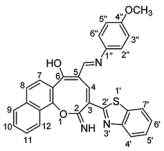

Yellowish orange crystals; (322 mg, 64%); mp 194–196 °C; IR (KBr, ν/cm^{-1}): 3300–3450 (OH, NH, broad), 3065 (aromatic CH), 2917 (aliphatic CH), 1630 (C=N), 1608 (C=C); ^{1}H NMR (500 MHz, DMSO-d_6): δ (ppm) 3.77 (s, 3H, OCH$_3$), 7.00 (dd, 2H, H-3″, H-5″, J = 2.10, 6.90, Hz), 7.48 (d, 1H, H-8, J = 8.90 Hz), 7.53 (dd, 1H, Ar–H, J = 7.00, 7.50 Hz), 7.59–7.64 (m, 2H, Ar–H), 7.70 (d, 1H, H-7, J = 8.90 Hz), 7.73 (dd, 1H, Ar–H, J = 1.50, 8.00 Hz), 7.78 (dd, 2H, H-2″, H-6″, J = 2.10, 6.90 Hz), 7.96 (d, 1H, H-7′, J = 8.20 Hz), 8.19 (d, 1H, H-4′, J = 7.60 Hz), 8.26 (d, 1H, H-9, J = 8.20 Hz), 8.38 (d, 1H, H-12, J = 8.20 Hz), 8.51 (d, 1H, CH=N, J = 2.10 Hz), 8.69 (d, 1H, H-4, J = 2.10 Hz), 11.89 (s, 1H, NH or OH), 12.96 (s, 1H, NH or OH); anal. calcd for $C_{30}H_{21}N_3O_3S$ (503.13): C, 71.55; H, 4.20; N, 8.34; S, 6.37%. Found: C, 71.59; H, 4.18; N, 8.33; S, 6.36%.

5-(((3-(benzo[*d*]thiazol-2-yl)-6-hydroxy-2-imino-2*H*-naphtho[1,2-*b*]oxocin-5-yl)methylene)amino)-3-(methylthio)-1*H*-pyrazole-4-carbonitrile (3c).

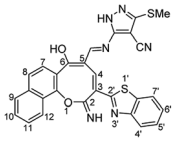

Yellowish orange crystals; (374 mg, 70%); mp 326–327 °C; IR (KBr, ν/cm^{-1}): 3380–3550 (OH, broad), 3450 (NH), 3226 (NH), 2215 (CN), 1630 (C=N), 1600 (C=C); ^{1}H NMR (500 MHz, DMSO-d_6): δ (ppm) 2.60 (s, 3H, SCH$_3$), 7.49–7.78 (m, 6H, Ar–H), 7.96 (d, 1H, Ar–H, J = 8.00 Hz), 8.15 (d, 1H, Ar–H, J = 8.50 Hz), 8.22 (d, 1H, Ar–H, J = 8.00 Hz), 8.41 (d, 1H, Ar–H, J = 8.50 Hz), 8.63 (d, 1H, Ar–H, J = 2.50 Hz), 8.76 (d, 1H, Ar–H, J = 2.50 Hz), 9.49 (s, 1H, NH or OH), 10.00 (s, 1H, NH or OH), 12.78 (s, 1H, NH or OH); EI-MS m/z (%): 534.82 [M$^+$] (48.94), 507.08 (40.21), 502.40 (32.33), 473.18 (16.44), 271.20 (54.74), 243.06 (68.660), 183.42 (77.08), 180.05 (100.00), 129.09 (58.57), 81.14 (58.28); anal. calcd for $C_{28}H_{18}N_6O_2S_2$ (534.09): C, 62.91; H, 3.39; N, 15.72; S, 11.99%. Found: C, 62.95; H, 3.35; N, 15.73; S, 11.96%.

5-(((4*H*-1,2,4-triazol-3-yl)imino)methyl)-3-(benzo[*d*]thiazol-2-yl)-2-imino-2*H*-naphtho[1, 2-*b*]oxocin-6-ol (3d).

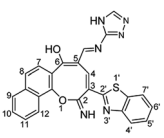

Canary yellow crystals; (255 mg, 55%); mp > 330 °C; IR (KBr, ν/cm^{-1}): 3200–3450 (OH, broad), 3424 (NH), 3209 (NH), 3059 (aromatic CH), 1601 (C=N), 1550 (C=C); ^{1}H NMR (500 MHz, DMSO-d_6): δ (ppm) 7.48 (d, 1H, H-8, J = 8.90 Hz), 7.54 (dd, 1H, Ar–H, J = 7.49, 7.51 Hz), 7.62 (dd, 2H, Ar–H, J = 6.50, 8.50 Hz), 7.66 (d, 1H, H-7, J = 8.90 Hz), 7.72 (dd, 1H, Ar–H, J = 7.00, 8.00 Hz), 7.82 (s, 1H, triazole), 7.95 (d, 1H, H-9, J = 8.20 Hz), 8.16 (d, 1H, H-7′, J = 7.60 Hz), 8.21 (d, 1H, H-4′, J = 7.60 Hz), 8.38 (d, 1H, H-12, J = 8.20 Hz), 8.61 (s, 1H, CH=N), 8.75 (s, 1H, H-4), 12.51 (s, 1H, NH or OH), 12.77 (s, 1H, NH or OH), 13.76 (s, 1H, NH or OH); EI-MS m/z (%): 464.29 [M$^+$] (100.00), 462.82 (17.73), 435.33 (13.86), 380.18 (13.32), 379.22 (9.70), 306.23 (18.92), 115.18 (17.33); anal. calcd for $C_{25}H_{16}N_6O_2S$ (464.11): C, 64.64; H, 3.47; N, 18.09; S, 6.90%. Found: C, 64.66; H, 3.42; N, 18.03; S, 7.01%.

5-(((1*H*-benzo[*d*]imidazol-2-yl)imino)methyl)-3-(benzo[*d*]thiazol-2-yl)-2-imino-2*H*-naph-tho[1,2-*b*]oxocin-6-ol (3e).

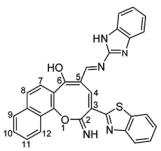

Yellow needles; (308 mg, 60%); mp 318 °C; IR (KBr, ν/cm^{-1}): 3270–3420 (OH, NH, broad), 3347 (NH), 3058 (aromatic CH), 1631 (C=N), 1590 (C=C); ^{1}H NMR (400 MHz, DMSO-d_6): δ (ppm) 7.22–7.56 (m, 7H, Ar–H), 7.67 (dd, 1H, Ar–H, J = 8.00, 8.50 Hz), 7.77 (d, 2H, Ar–H, J = 8.00 Hz), 8.01 (d, 1H, H-9, J = 8.00 Hz), 8.08 (dd, 2H, Ar–H, J = 8.00, 8.50 Hz), 8.43 (d, 1H, H-12, J = 8.00 Hz), 8.85 (s, 1H, CH=N), 9.18 (s, 1H, H-4), 12.01 (s, 1H, NH or OH), 12.53 (s, 1H, NH or OH), 13.00 (s, 1H, NH or OH); EI-MS m/z (%): 515.92 [M$^+$ + 2] (0.95), 514.32 [M$^+$ + 1] (1.03), 513.61 [M$^+$] (2.44), 398.31 (14.90), 397.25 (20.37), 355.34 (13.15), 354.30 (16.10), 337.26 (21.39), 339.26 (48.12), 337.26 (16.73), 40.20 (100.00); anal. calcd for $C_{30}H_{19}N_5O_2S$ (513.58): C, 70.16; H, 3.73; N, 13.64; S, 6.24%. Found: C, 70.18; H, 3.70; N, 13.62; S, 6.21%.

3-(benzo[*d*]thiazol-2-yl)-5-((3-hydroxy-5-imino-4,5-dihydro-1*H*-pyrazol-1-yl)methylene)-2-imino-2,5-dihydro-6*H*-naphtho[1,2-*b*]oxocin-6-one(6).

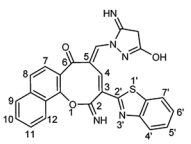

Yellow crystals; (240 mg, 50%); mp 310–311 °C; IR (KBr, ν/cm^{-1}): 3550–3420 (OH, broad), 3378 (NH), 3209 (NH), 3051 (aromatic CH), 2961, 2898 (aliphatic CH), 1636 (C=O), 1600 (C=N), 1596 (C=C); ^{1}H NMR (500 MHz, TFA): δ (ppm) 4.25 (s, 2H, CH$_2$), 7.43 (d, 1H, H-8, J = 8.90 Hz), 7.50 (d, 1H, H-7, J = 8.90 Hz), 7.65 (dd, 2H, Ar–H, J = 7.50, 8.00 Hz), 7.72 (dd, 1H, Ar–H, J = 7.00, 7.50 Hz), 7.79 (dd, 1H, Ar–H, J = 7.00, 7.50 Hz), 7.85 (d, 1H, H-7′, J = 8.20 Hz), 8.04 (d, 1H, H-4′, J = 7.50 Hz), 8.17 (d, 1H, H-9, J = 8.20 Hz), 8.54 (d, 1H, H-12, J = 8.20 Hz), 8.58 (d, 1H, CH=N, J = 1.40 Hz), 8.92 (d, 1H, H-4, J = 1.40 Hz); anal. calcd for $C_{26}H_{17}N_5O_3S$ (479.51): C, 65.13; H, 3.57; N, 14.61; S, 6.69%. Found: C, 65.16; H, 3.56; N, 14.65; S, 6.66%.

2-(benzo[*d*]thiazol-2-yl)-12-(piperidin-1-yl)-4,12-dihydro-3*H*-benzo[7,8]chromeno[4,3-*b*]pyridin-3-one (7).

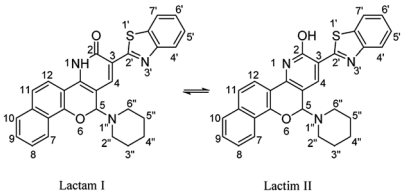

Note: both of keto and enol forms were only observed in NMR analyses due to the use of trifluoroacetic acid as solvent which might induce this tautomerization process.

Yellow crystals; (307 mg, 66%); mp > 330 °C; IR (KBr, ν/cm^{-1}): 3350–3460 (NH, broad), 3064 (aromatic CH), 2931–2816 (aliphatic CH), 1643 (C=O), 1604 (C=N), 1560 (C=C); ^{1}H NMR (500 MHz, TFA): δ (ppm) 1.49–2.16 (m, 12H, H-3″,4″,5″, I & II), 3.09–4.04 (m, 8H, H-2″, H-6″, I & II), 6.97 (s, 2H, H-4, I & II), 7.85 (dd, 2H, Ar–H, J = 7.49, 7.51 Hz, I & II), 7.92 (m, 4H, Ar–H, I & II), 7.97 (d, 4H, Ar–H, I & II) 8.05 (m, 2H, Ar–H, I & II), 8.12 (m, 2H, Ar–H, I & II), 8.22 (m, 2H, Ar–H, I & II), 8.29 (m, 2H, Ar–H, I & II), 8.46 (m, 2H, H-7, I & II), 9.03 (s, 2H, H-4, I & II); EI-MS m/z (%): 465.57 [M$^+$] (45.76), 462.54 (64.03), 331.08 (59.94), 315.14 (45.02), 99.57 (69.91), 83.35 (100.00), 59.43 (82.74), 55.20 (76.75); ^{13}C NMR (126 MHz, TFA): δ (ppm) 22.91, 23.34, 24.39, 24.68, 24.82, 48.52, 51.84, 52.98, 68.60, 91.64, 105.22, 109.30, 114.16, 114.32, 119.54, 120.53, 122.93, 123.98, 124.69, 124.90, 125.15, 125.38, 125.62, 128.92, 130.94, 131.22, 131.39, 131.75, 132.75, 132.93, 133.06, 133.21, 133.92, 134.22, 135.79, 137.48, 140.42, 140.66, 141.64, 142.14, 144.41, 146.13, 148.36, 153.73, 168.88; anal. calcd for $C_{28}H_{23}N_3O_2S$ (465.57): C, 72.24; H, 4.98; N, 9.03; S, 6.89%. Found: C, 72.22; H, 4.99; N, 9.01, S, 6.87%.

(1-Amino-5-(benzo[*d*]thiazol-2-yl)-6-imino-1,6-dihydropyridin-3-yl)(1-hydroxynaphthal en-2-yl)methanone (8).

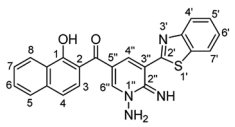

Pale yellow crystals; (301 mg, 73%); mp 240–241 °C; IR (KBr, ν/cm^{-1}): 3460–3100 (OH, NH$_2$ broad), 3129 (NH), 1648 (C=O), 1628 (C=N), 1599 (C=C); ^{1}H NMR (500 MHz, DMSO-d_6): δ (ppm) 7.29 (s, 2H, NH$_2$), 7.51 (d, 1H, H-3, J = 8.20 Hz), 7.57 (dd, 1H, H-6′, J = 7.49, 7.51 Hz), 7.61–7.65 (dd, 2H, Ar–H), 7.66 (d, 1H, H-4′, J = 8.90 Hz), 7.73 (dd, 1H, H-5′, J = 7.49, 7.51 Hz), 7.96 (d, 1H, H-4, J = 8.20 Hz), 8.22 (d, 1H, H-8, J = 8.20 Hz), 8.39 (d, 1H, H-5, J = 8.20 Hz), 8.68 (d, 1H, H-4″, J = 1.40 Hz), 8.78 (s, 1H, H-6″), 10.18 (brs, 1H, OH), 12.30 (s, 1H, NH); EI-MS m/z (%): 412.34 [M$^+$] (8.22), 350.34 (42.07), 305.04 (73.80), 240.95 (100.00), 221.44 (77.21), 107.52 (50.84), 83.05 (76.40); ^{13}C NMR (126 MHz, DMSO-d_6): δ (ppm) 114.79, 114.91, 119.21, 121.40, 122.24, 123.21, 123.56, 124.73, 126.08, 126.17, 126.83, 127.16, 127.57, 129.86, 133.17, 136.64, 139.87, 144.94, 151.63, 151.84, 158.63, 163.06, 191.91; anal. calcd for $C_{23}H_{16}N_4O_2S$ (412.47): C,

66.98; H, 3.91; N, 13.58; S, 7.77%. Found: C, 66.95; H, 3.93; N, 13.59; S, 7.79%.

(8-(Benzo[*d*]thiazol-2-yl)-2-thioxo-2,3-dihydro-[1,2,4]triazolo [1,5-*a*]pyridin-6-yl)(1-hydroxynaphthalen-2-yl)methanone (10).

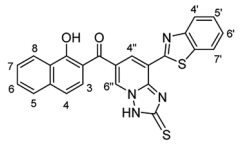

Orange crystals; (241 mg, 53%); mp 264 °C; IR (KBr, ν/cm^{-1}): 3450–3300 (OH, broad), 3293 (NH), 3054 (aromatic CH), 1637 (C=N), 1593 (C=C); ^{1}H NMR (500 MHz, DMSO-d_6): δ (ppm) 7.48–7.50 (m, 2H, Ar–H), 7.57 (dd, 1H, H-7, J = 7.00, 8.00 Hz), 7.63 (dd, 1H, Ar–H, J = 7.00, 8.50 Hz), 7.67 (dd, 1H, J = 1.50, 7.60 Hz), 7.73 (dd, 1H, H-6, J = 7.00, 8.00 Hz), 7.96 (d, 1H, H-5, J = 8.20 Hz), 8.14 (dd, 2H, Ar–H, J = 8.00, 9.00 Hz), 8.38 (d, 1H, Ar–H, J = 8.20 Hz), 8.40 (d, 1H, H-4″, J = 2.00 Hz), 8.59 (d, 1H, H-6″, J = 2.00 Hz), 8.76 (brs, 2H, NH_2), 12.85 (s, 1H, OH); EI-MS m/z (%): 471.08 [M^+] (14.29), 420.45 (18.15), 263.38 (19.92), 147.26 (37.62), 102.65 (21.94), 97.34 (38.44), 67.14 (100.00), 60.16 (52.60), 53.36 (84.10); anal. calcd for $C_{24}H_{17}N_5O_2S_2$ (471.55): C, 61.13; H, 3.63; N, 14.85; S, 13.60%. Found: C, 61.15; H, 3.64; N, 14.84 S, 13.56%.

Computational prediction of biological activities of oxocine derivatives 3a–e and 6

The 2D chemical structures of the oxocine derivatives **3a–e** and **6** were drawn using both ChemDoodle[36] and Marvin Sketch (ChemAxon, Version 18.30). After that SwissADME predictor software (http://www.swissadme.ch/) was used to convert the 2D structures into SMILEY mode.[37] The biological activities of the synthesized products were predicted using PASS online software. The main target of PASS (prediction of activity spectra for biologically active substances) is prediction of the most probable kind of biological activity from the chemical structure. It reflects all biological activities that arise from interactions with biological entities among the compounds from the viable database. In this study, PASS develops prediction of biological activities with the probabilities of Pa (to be active) and Pi (to be inactive) values.[38]

Conflicts of interest

The authors have no conflict of interest to mention.

References

1 J. Cossy, M. Brimble and M. Cordes, *Synthesis of Saturated Oxygenated Heterocycles*, Springer, 2014.
2 B. Harrison and P. Crews, *J. Org. Chem.*, 1997, **62**, 2646–2648.
3 A. Arnone, G. Nasini, W. Panzeri, O. V. d. Pava and L. Malpezzi, *J. Nat. Prod.*, 2007, **71**, 146–149.
4 W. Steglich, *Pure Appl. Chem.*, 1989, **61**, 281–288.
5 L.-c. Fu, X.-a. Huang, Z.-y. Lai, Y.-j. Hu, H.-j. Liu and X.-l. Cai, *Molecules*, 2008, **13**, 1923–1930.
6 T. Ghosh, *Synth. Commun.*, 2018, **48**, 1338–1345.
7 L. Liang, E. Li, X. Dong and Y. Huang, *Org. Lett.*, 2015, **17**, 4914–4917.
8 T. Ghosh, *New J. Chem.*, 2017, **41**, 2927–2933.
9 R. K. Boeckman, J. Zhang and M. R. Reeder, *Org. Lett.*, 2002, **4**, 3891–3894.
10 S. K. Chattopadhyay, S. Karmakar, T. Biswas, K. Majumdar, H. Rahaman and B. Roy, *Tetrahedron*, 2007, **63**, 3919–3952.
11 M. Bratz, W. H. Bullock, L. E. Overman and T. Takemoto, *J. Am. Chem. Soc.*, 1995, **117**, 5958–5966.
12 K. Nicolaou, D. McGarry, P. Somers, B. Kim, W. Ogilvie, G. Yiannikouros, C. Prasad, C. Veale and R. Hark, *J. Am. Chem. Soc.*, 1990, **112**, 6263–6276.
13 S. Ma and E.-i. Negishi, *J. Org. Chem.*, 1994, **59**, 4730–4732.
14 N. Ortega, T. Martín and V. S. Martín, *Org. Lett.*, 2006, **8**, 871–873.
15 S. K. Mandal and S. C. Roy, *Tetrahedron*, 2007, **63**, 11341–11348.
16 M. Sasaki, A. Hashimoto, K. Tanaka, M. Kawahata, K. Yamaguchi and K. Takeda, *Org. Lett.*, 2008, **10**, 1803–1806.
17 M. A. Ibrahim, *ARKIVOC*, 2008, (xvii), 192–204.
18 J. Li, J. M. Suh and E. Chin, *Org. Lett.*, 2010, **12**, 4712–4715.
19 H.-H. Liao and R.-S. Liu, *Chem. Commun.*, 2011, **47**, 1339–1341.
20 A. Thakur and J. Louie, *Acc. Chem. Res.*, 2015, **48**, 2354–2365.
21 G. Kim, T. i. Sohn, D. Kim and R. S. Paton, *Angew. Chem., Int. Ed.*, 2014, **53**, 272–276.
22 M. Ibrahim, N. El-Gohary, S. Ibrahim and S. Said, *Chem. Heterocycl. Compd.*, 2015, **50**, 1624–1633.
23 M. A. Ibrahim and T. E.-S. Ali, *Turk. J. Chem.*, 2015, **39**, 412–425.
24 S. P. Alexander, E. Kelly, N. Marrion, J. A. Peters, H. E. Benson, E. Faccenda, A. J. Pawson, J. L. Sharman, C. Southan and O. P. Buneman, *Br. J. Pharmacol.*, 2015, **172**, 5729–5743.
25 M. Frisch, G. Trucks, H. Schlegel, G. Scuseria, M. Robb, J. Cheeseman, G. Scalmani, V. Barone, B. Mennucci and G. Petersson, *Gaussian 09, Revision D.01*, Gaussian, Inc., Wallingford CT USA, 2009.
26 A. D. Becke, *Phys. Rev. A: At., Mol., Opt. Phys.*, 1988, **38**, 3098–3100.
27 C. Lee, W. Yang and R. G. Parr, *Phys. Rev. B: Condens. Matter Mater. Phys.*, 1988, **37**, 785–789.
28 N. Godbout, D. R. Salahub, J. Andzelm and E. Wimmer, *Can. J. Chem.*, 1992, **70**, 560–571.
29 S. Gupta and J. M. Khurana, *Green Chem.*, 2017, **19**, 4153–4156.
30 M. A. Ibrahim and A.-S. Badran, *ARKIVOC*, 2018, (vii), 214–224, DOI: 10.24820/ark.5550190.p010.745.
31 A good agreement was found between the experimental and predicted IR spectra of compound **3a** which support the reliability of the calculated results. Predicted IR absorptions: 3450 cm^{-1} (OH), 3280 cm^{-1} (NH), 33105 cm^{-1} (aromatic CH), 1608 cm^{-1} (C=N), 1530 cm^{-1} (C=C) (see ESI†).
32 S. E. Koops, B. C. O'Regan, P. R. Barnes and J. R. Durrant, *J. Am. Chem. Soc.*, 2009, **131**, 4808–4818.

33 Q.-H. Yao, L. Shan, F.-Y. Li, D.-D. Yin and C.-H. Huang, *New J. Chem.*, 2003, **27**, 1277–1283.
34 M. Al-Eid, S. Lim, K. Park, B. Fitzpatrick, C. Han, K. Kwak, J. Hong and G. Cooke, *Dyes Pigm.*, 2014, **104**, 197–203.
35 X. Liu, Z. Cao, H. Huang, X. Liu, Y. Tan, H. Chen, Y. Pei and S. Tan, *J. Power Sources*, 2014, **248**, 400–406.
36 M. C. Burger, *J. Cheminf.*, 2015, **7**, 35.
37 A. Daina, O. Michielin and V. Zoete, *Sci. Rep.*, 2017, **7**, 42717.
38 S. Parasuraman, *J. Pharmacol. Pharmacother.*, 2011, **2**, 52–53.